



Content-Based Medical Image Retrieval System for Skin Melanoma Diagnosis Based on Optimized Pair-Wise Comparison Approach

Narendra Kumar Rout¹ · Mitul Kumar Ahirwal² · Mithilesh Atulkar¹

Received: 16 July 2021 / Revised: 20 August 2022 / Accepted: 27 September 2022 / Published online: 17 October 2022
© The Author(s) under exclusive licence to Society for Imaging Informatics in Medicine 2022

Abstract

Medical image analysis for perfect diagnosis of disease has become a very challenging task. Due to improper diagnosis, required medical treatment may be skipped. Proper diagnosis is needed as suspected lesions could be missed by the physician's eye. Hence, this problem can be settled up by better means with the investigation of similar case studies present in the healthcare database. In this context, this paper substantiates an assistive system that would help dermatologists for accurate identification of 23 different kinds of melanoma. For this, 2300 dermoscopic images were used to train the skin-melanoma similar image search system. The proposed system uses feature extraction by assigning dynamic weights to the low-level features based on the individual characteristics of the searched images. Optimal weights are obtained by the newly proposed optimized pair-wise comparison (OPWC) approach. The uniqueness of the proposed approach is that it provides the dynamic weights to the features of the searched image instead of applying static weights. The proposed approach is supported by analytic hierarchy process (AHP) and meta-heuristic optimization algorithms such as particle swarm optimization (PSO), JAYA, genetic algorithm (GA), and gray wolf optimization (GWO). The proposed approach has been tested with images of 23 classes of melanoma and achieved significant precision and recall. Thus, this approach of skin melanoma image search can be used as an expert assistive system to help dermatologists/physicians for accurate identification of different types of melanomas.

Keywords Content-based medical image retrieval system (CBMIR) · Skin melanoma · Analytic hierarchy process (AHP) · Particle swarm optimization (PSO) · Jaya algorithm

Introduction

After the post-classical era, computer-aided diagnosis (CAD) systems have been used to support medical professionals by analyzing the conspicuous section of any specific lesions [1, 2]. As the function of the human body is most complex, medical specialists must have to evaluate and analyze the medical images [3]. Improved diagnosis is based on the

previous investigation of related and similar medical cases to find the best possible treatment for a patient. Present-day disease diagnostic methods involve a lot of imaging data and techniques. A huge amount of visual information is collected through these modern imaging techniques like computed tomography (CT) scan [4], nuclear imaging, 3D imaging optical projection tomography (OPT), optical biopsy, magnetic resonance imaging (MRI) scan, nuclear medicine positron emission tomography (PET), angiography test for clear diagnosis, and treatment [3, 5].

The improved treatment through various medical imaging diagnosis techniques seeks to localize the various internal and hidden abnormalities inside the organs of the human body. Hence, it takes more time to retrieve the homogeneous images from the large medical image database containing visual information. To alleviate this problem, content-based medical image retrieval (CBMIR) system is a tool to assist physicians in searching past similar medical records from the medical database. This helps in taking the right decision for accurate treatment.

✉ Mitul Kumar Ahirwal
ahirwalmitul@gmail.com
Narendra Kumar Rout
narendrarout@gmail.com
Mithilesh Atulkar
matulkar.mca@nitrr.ac.in

¹ Department of Computer Application, NIT, Raipur, C.G. 492010, India

² Department of Computer Science and Engineering, MANIT, Bhopal, M.P. 462003, India

In the offline process of CBMIR system, a feature vector is created for every image of the medical database after feature extraction. Then, in the online process, the feature is extracted from the query image and compared with the feature vector found from the offline process to measure the similarity of the corresponding resultant images. Many known feature extraction methods based on color are color moments [6, 7], color histogram [8], and color-correlogram [9]. Moment of invariants [10], eccentricity, solidity, circularity, and Zernike moments [11, 12] are different shape feature extraction techniques. The frequently used texture feature extraction methods are first-order-feature, gray-level co-occurrence matrix (GLCM) [13, 14], and discrete and wavelet transform (DWT) [15]. Many other low- and high-level image features are also discussed in available literature [16–18].

The efficient CBMIR systems were supported through classification methods over brain MRI images [19, 20], histopathological medical images of breast microscopic tissues [21], lung CT images [22, 23], and clinical mammogram images [24], for better retrieval efficiency. Many of the researches on the clinical study are focused on multiple feature-based retrieval systems. A medical image retrieval system has been developed with the shape–texture descriptors on lung image database [25], texture-color features on pigmented lesion dermoscopic database [26], and different texture features on lung CT image database [22]. For achieving better accuracy from the retrieval system, researchers have adapted an optimized feature-based medical image retrieval system. In Renita and Christopher [27], the author examined the optimized approach with grey-wolf optimization (GWO)-based support vector machine (SVM) to retrieve images from the classification of huge CT scan image database. An efficient retrieval system has been studied through the optimal feature selection approach of fisher criterion and genetic algorithm (GA) for classifying lung CT images [22]. Hashing approach is utilized on retrieval system for classifying histopathological medical images of breast microscopic tissues [21]. In Murala and Wu [20], the retrieval system for (Open Access Series of Imaging Studies-MRI) OASIS-MRI database, (National Electrical Manufacturers Association-CT) NEMA-CT database, and VIA/I–ELCAP database for CT and MRI images have been used with texture features like local mesh pattern. Similar to this, the local neighborhood-based wavelet feature descriptor [23] also helps for analyzing neighboring pixels of an image. The promising hybrid approach was established for the efficient classification of brain MRI images [19]. An automated system for retrieving similar medical images from the large database to help physicians in making their decisions is developed in Shamna et al. [28]. Various skin disease classification and detection have also been performed for better diagnosis of the disease [29–31].

For exploring such CBMIR system, image classification based on feature extraction and image indexing is becoming challenges due to individual characteristics among different image classes [27], which yields low retrieval performance [2]. To resolve this issue, multiple images features color, shape, and texture are mixed for providing better classification result. This classification result can be more noteworthy by assigning appropriate weights among features. It has been found that the analytical hierarchical process (AHP) is a pairwise comparison approach employed in image features for proper distribution of weight percentage [32]. AHP helps in reducing the semantic gap of the semantic learning process [30, 33]. To achieve better performance of retrieval result, several comparisons and expertise are required to choose the proper intensity importance value among features. Hence, finding an appropriate optimal weight is a matter of great concern for complicated medical images.

Several literature studies in many areas have focused on the successful combination of AHP with global optimization algorithms for resolving the problems. An efficient method using AHP with an evolutionary GA approach provides a better weighting calculation of the energy performance level in residential buildings [33]. The promising combination of AHP-GA solves the weight intensity problem in achieving optimal weights [33]. The hybrid concept with nature-inspired optimization like AHP-particle swarm optimization (PSO) has been implemented in the information security system to get remarkable final risk performance result [34]. Also, this approach establishes a hierarchical structure of risk assessment with a better risk control plan for the information security system [35, 36].

In biomedical applications, the ideal feature of PSO facilitates within the indexing process of CBIR analyzing over DermAtlas image database [37] and keeps on obtaining significant accuracy as against the other optimization techniques [36]. The author [38] addresses a model based on AHP with PSO for the selection of an optimal supplier system. The GWO approach leads to an improved result in image processing applications [39]. It has been found that the Jaya algorithm (JAYA) shows significant accuracy in the facial recognition field [40] as well as brain MRI medical images [41].

A modified active disturbance rejection control (M-ADRC) system is proposed to resolve the time-delay issues in ADRC. To overcome the time delay factor, the M-ADRC system has been proposed to tune with the multi-objective quasi oppositional Jaya algorithm (MOQO-JAYA) and at the end achieves a successful outcome with the support of AHP [42].

From the above literature review and best of the author's knowledge, the combination of AHP and the bio-inspired based algorithm has not yet been reported in the field of CBMIR systems. Therefore, in this paper, an attempt has

been made to utilize the advantages of global optimizers with the analytic hierarchy process for enhancing the efficiency of CBMIR systems.

The key contributions of the paper are as follows:

- A new approach for automatic and dynamic weight selection for image features has been proposed and tested with a real database of skin melanoma images. The proposed system assists the physicians for the right diagnosis after identifying the type of disease.
- Analytical hierarchical process (AHP) and several swarm optimization algorithms have been utilized to automate the feature weight selection process.
- A complete content-based medical image retrieval (CBMIR) system has been developed for skin melanoma diagnosis.

This gives huge motivation towards the development of an expert system that assists the physicians for the right diagnosis after identifying the type of diseases from the clinical image database using modern image recognition approaches. The proposed CBMIR model uses a method of feature extraction and assigning dynamic weights to the low-level extracted features based on the individual characteristics of the searched images. The novelty of the proposed model is in basing the optimal weights assigned to the features of the searched image instead of applying common or average weights.

The outline structure of the paper proceeds as follows: the introduction of issues with the background studies on CBMIR, AHP method, and various optimization approaches is discussed in “Introduction”. Materials and the basic concepts of pair-wise comparison methods and optimization algorithms are presented in “Materials and Methodology”. “Proposed formulation for optimized AHP” deals with the procedure of the proposed model. Simulation results are provided in “Simulation and Result Analysis” and discussion in “Discussion”. In the end, the conclusion of the present study is provided in “Conclusion”.

Materials and Methodology

Dataset

In this research study, the standard skin lesion database (DermNet) for melanoma detection [43–45] has been used. This database consists of 23 different types of skin melanoma disease images. The images are stored in JPEG format, all are color images having red, green, and blue channels. The resolutions of images are different, and images are also of normal quality (not extremely high

resolution). Database is divided into two groups: the first includes a total of 15,592 numbers of images (training group), and the second includes 4002 numbers of images (later called testing group). For experiments and simulations of proposed method, 100 random images were taken from each class (total 2300 images) for training, and 10 random images were taken from each class (230 images) for testing. Database can be downloaded from <https://www.kaggle.com/datasets/shubhamgoel27/dermnet>. Samples of images of each class in the melanoma database are shown in Table 1.

AHP

The analytical hierarchical process is based on decision-making theory, which is also known as the pair-wise comparison method [32, 46]. In this, the main steps are hierarchy construction for criterion, calculation of weights for criterion (here, image features are considered as criterion), and their consistency checking. At first, the top of the hierarchical structure is constructed with the main aim of retrieving similar images. As per the contents of an image, the associated criterion value is selected in the second step, and at the third step of the process, images are retrieved for database images considered as each of the alternatives.

During the process of weight calculation, a pair-wise comparison is established among individual image features (color, shape, and texture). Then, ranking of images is determined from the calculated feature’s weight. In this calculation, first, a pair-wise comparison matrix A is supplemented with the value as $(a_{ij})_{n \times n}$. The possible values of relative intensity importance (a_{ij}) in a given criterion is established. Then, there is a comparison made between two feature vectors (i) and (j) with respect to criteria U based on the nature of image. These relative intensity importance (scaling) values are shown in Table 2. The pair-wise comparison matrix, $A = (a_{ij})_{n \times n}$ is represented in Eq. (1) as follows:
























$$A = \begin{bmatrix} a_{11} & a_{12} & a_{13} \\ a_{21} & a_{22} & a_{23} \\ a_{31} & a_{32} & a_{33} \end{bmatrix}, \quad (1)$$

where n is the number of alternatives (features) and the procedure presents important characteristics as in Eq. (2):

$$\left. \begin{array}{l} a_{ij} = 1/a_{ji} \\ a_{ii} = 1 \end{array} \right\} \quad (2)$$

After the completion of matrix, the features’ weights are evaluated by using eigenvalue method (λ_{\max}). The process of eigenvalue method is analyzed as follows:

Table 1 Samples of images of each class with names of skin melanoma

					
(1) Acne and Rosacea	(2) Actinic Keratosis Basal Cell Carcinoma and other Malignant Lesions	(3) Atopic Dermatitis	(4) Bullous Disease	(5) Cellulitis Impetigo and other Bacterial Infections	(6) Eczema
					
(7) Exanthems and Drug Eruptions	(8) Hair Loss Alopecia and other Hair Diseases	(9) Herpes HPV and other STDs	(10) Light Diseases and Disorders of Pigmentation	(11) Lupus and other Connective Tissue diseases	(12) Melanoma Skin Cancer Nevi and Moles
					
(13) Nail Fungus and other Nail Disease	(14) Poison Ivy Photos and other Contact Dermatitis	(15) Psoriasis pictures Lichen Planus and related diseases	(16) Scabies Lyme Disease and other Infestations and Bites	(17) Seborrheic Keratoses and other Benign Tumors	(18) Systemic Disease
					
(19) Tinea Ringworm Candidiasis and other Fungal Infections	(20) Urticaria Hives	(21) Vascular Tumors	(22) Vasculitis	(23) Warts Molluscum and other Viral Infections	

In the pair-wise matrix (A), the products M of elements per row are computed with the basis of concerned formula given in Eq. (3):

$$M_i = \prod_j^N a_{ij}, \tag{3}$$

Table 2 Relative importance factor (scales) for pair-wise comparison matrix [29, 43]

Intensity of importance (a_{ij})	Definition
1	i has the same importance as j with respect to U
3	i has slightly more importance than j with respect to U
5	i has more importance than j with respect to U
7	i has a lot more importance than j with respect to U
9	i totally dominates j with respect to U
2,4,6,8	Intermediate values between the two adjacent judgments

where ($i = 1, 2, 3 \dots N$), N is the rank of matrix (A). However, the ranking (N) of pair-wise matrix (A) is established over the eigenvalue and vector (V) as obtained the Eq. (4):

$$V_i = \sqrt[N]{M_i}. \tag{4}$$

For proper weight distribution, the normalization of selected eigenvector is used for calculating relative feature’s weight, as per the content of image. After the process of assigning weights, the consistency check is determined for justifying the user’s judgment. The consistency index (CI) and consistency ratio (CR) are evaluated with Eqs. (5) and (6), respectively:

$$CI = (\lambda_{\max} - N)/(N - 1), \tag{5}$$

$$CR = CI/RI. \tag{6}$$

where RI defines the random index, and its value depends on the matrix dimension. If the condition of consistency ratio

is $CR \leq 0.1$, the selected intensity importance is considered, and otherwise, the relative intensity importance (scale) is to be chosen from the set of values [47, 48].

Optimization Algorithms

GA

The three main phases of GA include selection, crossover, and mutation over chromosomes (potential solutions) to transform the old population into a newly updated population. The fitness value for an individual solution is determined by the cost function for identifying the best solution from the population. The basic strategy of GA is based on providing a better individual selection to generate improved individuals in the next generation. The floating-point representation used in real GA for chromosomes improves the efficiency of GA. The real GA uses the arithmetic crossover and arithmetic mutation operators [49]. The crossover operation is represented by Eq. (7):

$$\left. \begin{aligned} C_x^{g+1} &= a \cdot (C_x^g) + (1 - a) \cdot (C_y^g) \\ C_y^{g+1} &= (1 - a) \cdot (C_x^g) + a \cdot (C_y^g) \end{aligned} \right\} \quad (7)$$

where C_x^g and C_y^g are the randomly chosen chromosomes with more than 50% fitness value. C_x^{g+1} and C_y^{g+1} are the next generation of chromosomes produced as linear mapping of parent chromosomes. The value of random number a is in between 0 and 1.

GA selects the chromosomes according to their respective fitness value using the tournament selection method. When the values of decision variables converging to optimal or the maximum iteration are reached, the whole process is terminated.

PSO

The robust stochastic PSO technique [36] is very widely used due to its excellent prompt convergence action producing an improved optimized solution. The flexibility of PSO with other computational intelligence approaches is used to achieve better performance in a particular period [36, 38].

In the course of food hunting, the optimal fitness value of PSO algorithm is dependent on moving directions and covered distance from the index velocity among every swarm particle. The earlier respective personal best position (pbest) and global best position (gbest) produced by an individual swarm determine the optimal value. The corresponding velocity and position of each particle can be updated showed in Eqs. (8) and (9), respectively.

$$\begin{aligned} V_{ij}(t+1) &= W * V_{ij}(t) \\ &+ c1 * r1 * (X_{pbest}(t) - X_{ij}(t)) \\ &+ c2 * r2 * (X_{gbest}(t) - X_{ij}(t)) \end{aligned} \quad (8)$$

$$X_{ij}(t+1) = X_{ij}(t) + V_{ij}(t+1), \quad (9)$$

where t is known as iteration. The velocity V_{ij} and position P_{ij} are representing the i th particle on the j th dimension respectively. The corresponding positions X_{pbest} and X_{gbest} are determined from pbest and gbest of the same particle in community along the j th dimension. The global exploration and local exploitation remains balanced with the inertia of weight W . The random functions $r1$ and $r2$ are in the interval $[0, 1]$. b is introduced as constraint factor for checking the velocity weight, considering the value of 1; the positive constants $c1$ and $c2$ describing personal and social learning factors, set as 1.5 and 2. b is called constraint factor that checks the velocity weight, considering the value of 1; $c1$ and $c2$ are positive constants describing personal and social learning factors, set as 1.5 and 2.

The optimal value is derived from the earlier respective personal best position (pbest) and global best position (gbest) made by each swarm particle during food hunting. The entire process is terminated only when it achieves global best (gbest) or values of decision variables converge to optimal weight.

GWO

As the name suggests, the GWO technique is based on the hunting life of wolf [39]. As per the fitness, the food hunting behavior of the GWO algorithm consists of a hierarchy of leadership [50] organized in Alpha (α), Beta (β), Delta (δ), and Omega (ω). The entire theme of this algorithm follows the elements, such as searching (exploration), surrounding (exploration), and attacking a feed (exploitation).

The method of hunting along with surrounding the feed or prey by grey wolves can be expressed concerned to Eqs. (10) and (11), as follows:

$$\vec{D} = \left| \vec{C} \cdot \vec{X}_{feed(t)} - \vec{X}_{grw(t)} \right|, \quad (10)$$

$$\vec{X}_{grw(t+1)} = \vec{X}_{feed(t)} - \vec{A} \cdot \vec{D}. \quad (11)$$

The current position vector of a feed (prey) and a grey wolf are denoted as $\vec{X}_{feed(t)}$ and $\vec{X}_{grw(t)}$ respectively at the current iteration. The grey wolves are separated from the feed apart from the distance \vec{D} . \vec{A} and \vec{C} signify coefficient vectors, which are shown in Eqs. (12) and (13):

$$\vec{A} = 2\vec{a} \cdot \vec{R}_1 - \vec{a}, \quad (12)$$

$$\vec{C} = 2 \cdot \vec{R}_2. \quad (13)$$

From the relevant equations, vector \vec{a} moves slowly down from 2 to 0 as the iterations progressed. The range of values in random vectors \vec{R}_1 and \vec{R}_2 is 0 and 1.

While hunting, the three best possible solutions *lpha*, *beta*, *delta* are saved and set. Following these three desired solutions, one more solution *Omega* tends to get the changed position. Subsequently, the position resetting by the grey wolves is derived in mathematical Eqs. (14)–(16):

$$\left. \begin{aligned} \vec{D}_{\text{Alpha}} &= \left| \vec{C}_1 \cdot \vec{X}_{\text{Alpha}} - \vec{X} \right| \\ \vec{D}_{\text{Beta}} &= \left| \vec{C}_2 \cdot \vec{X}_{\text{Beta}} - \vec{X} \right| \\ \vec{D}_{\text{Delta}} &= \left| \vec{C}_3 \cdot \vec{X}_{\text{Delta}} - \vec{X} \right| \end{aligned} \right\}, \quad (14)$$

$$\left. \begin{aligned} \vec{X}_1 &= \vec{X}_{\text{Alpha}} - \vec{A}_1 \cdot \vec{D}_{\text{Alpha}} \\ \vec{X}_2 &= \vec{X}_{\text{Beta}} - \vec{A}_2 \cdot \vec{D}_{\text{Beta}} \\ \vec{X}_3 &= \vec{X}_{\text{Delta}} - \vec{A}_3 \cdot \vec{D}_{\text{Delta}} \end{aligned} \right\}, \quad (15)$$

$$\vec{X}_{t+1} = \frac{\vec{X}_1 + \vec{X}_2 + \vec{X}_3}{3}. \quad (16)$$

At a distance of \vec{D}_{Alpha} , \vec{D}_{Beta} , \vec{D}_{Delta} , the feed (prey) is present from the current individual fitness solutions alpha, beta, delta. As stated by the equations, the random vectors are identified as \vec{C}_1 , \vec{C}_2 , \vec{C}_3 and in addition to this, the position vectors \vec{X}_{Alpha} , \vec{X}_{Beta} , \vec{X}_{Delta} are represented for the fitness solutions alpha, beta, and delta, respectively. Another position vector of current solution sets as \vec{X} . After calculating the distance, the new modified position vectors of current fitness solutions are found from Eqs. (16) and (17) in respect of t iterations. The vectors \vec{A}_1 , \vec{A}_2 , \vec{A}_3 are random coefficient vectors. The similar fashion of explanation from Eqs. (15) to (17) is applied in another grey wolf, *Omega*.

JAYA

The Jaya algorithm [51] makes an attempt to reach closer at desirable solutions and takes a turn to avoid from the poor solution of a particular problem [52]. For best optimal results, Jaya algorithm takes the short period of time with minimal effort [53]. It can be seen that Jaya algorithm has achieved desirable accuracy in several areas of applications due to its successful adoption [40, 41]. In this algorithm, the value of both random numbers $r_{1,v,k}$ and $r_{2,v,k}$ in the objective function, $W_{\max}(x)$ ranges between 0 and 1. The variables p and D are considered as the population size ($w = 1, 2, \dots, p$) and design variable ($v = 1, 2, \dots, D$) respectively. The entire population provides the best value, i.e., $W_{\text{best}}(x)$, and the worst value, i.e., $W_{\text{worst}}(x)$. The value of $X_{v,w,k}$ can then be

later updated as stated in Eq. (17), where the variable w^{th} candidate carries the value of the variable v^{th} at k th number of iterations:

$$X'_{v,w,k} = X_{v,w,k} + r_{1,v,k}(X_{v,\text{best},k} - |X_{v,w,k}|) - r_{2,v,k}(X_{v,\text{worst},k} - |X_{v,w,k}|). \quad (17)$$

$X_{v,\text{best},k}$ refers as the best candidate and $X_{v,\text{worst},k}$ refers as worst candidate for the variable v . The value of $r_{1,v,k}(X_{v,\text{best},k} - |X_{v,w,k}|)$ informs to ensure the best result. Also, the status of worst result can be notified from the value of $-r_{2,v,k}(X_{v,\text{worst},k} - |X_{v,w,k}|)$. The best value of objective function estimates the new modified value $X'_{v,w,k}$ [51].

Proposed formulation for optimized AHP

The workflow of the proposed CBMIR system with AHP enhanced by optimization techniques used in skin melanoma medical images is illustrated in Fig. 1. In the proposed OPWC retrieval system, the concept of a pair-wise comparison method for appropriate weight percentage distribution among features has been implemented. Weight percentage is evaluated using the intensity importance value entered by a user based on individual properties of an image; this is a general and manual approach. This will not provide better consistency and leads to inaccuracy. To get better consistent accuracy, there is a need for a user-free method that is independent of the experiment's presumptions and biases. For this reason, the present study proposes to utilize OPWC for getting optimum weight, having no user assistance.

The main goal of the optimization algorithm is to attain optimal weight. The objective function of this study highlights the goal of specified optimization algorithms, where the pair-wise comparison has been implemented for solving the problem. When entering the weight intensity value to the fitness function (f), it identifies the suitable combination among features. This relevant combination is established on the best recall value of the proposed model. In this regard, the weight percentage is derived, among features of the individual characteristic of medical image. The respective weight percentage of three different features, color, shape, and texture are w_c , w_s , and w_t specified as weight vector $W = [w_c w_s w_t]$. The optimized weight value of individual feature is subjected to consistency index (CI), $CI < 0.1$, and summation of $w_c + w_s + w_t = 1$. Reason behind keeping CI value less than 0.1 (10%) is proper selection of judgment matrix. If the consistency index is $CI \leq 0.1$, then the selected intensity importance is followed, and if not, relative intensity importance will be chosen again. This is the definition given by Dr. Thomas Satya in Saaty [47].

The above said fitness function is given in Eq. (18):

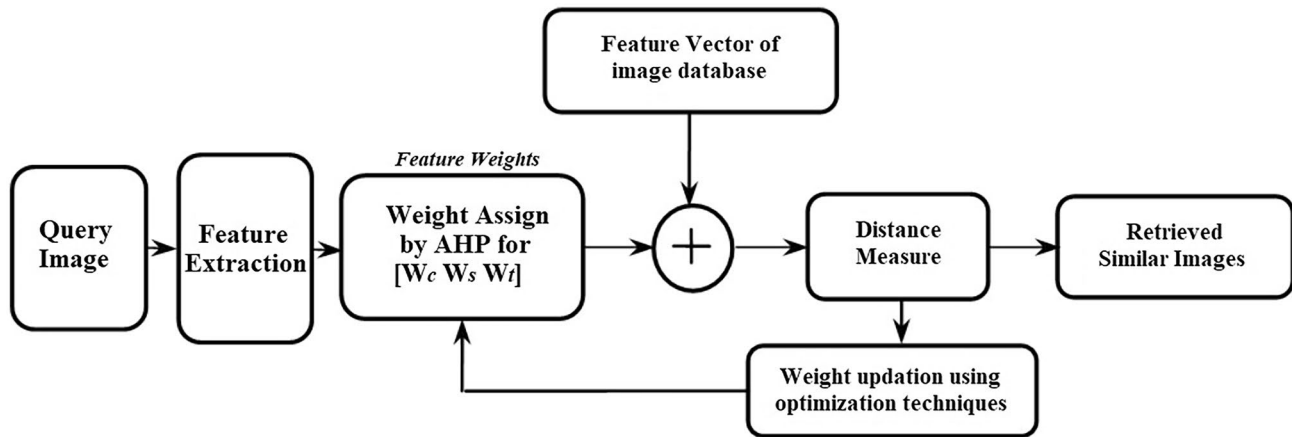


Fig. 1 Proposed OPWC approach for generating optimal feature weights

$$\left. \begin{aligned} &fitness = f(W) \\ &subject\ to: w_c + w_s + w_t = 1 \\ &CI < 0.1 \end{aligned} \right\} \quad (18)$$

The pseudocode of proposed OPWC algorithm is given below.

Pseudocode: Optimized-AHP

Input: Initial Population and image features.

Output: Optimal weights and Recall value.

Randomly initialize the intensity importance as solutions

While Maximum iteration reached

Calculate fitness for each solutions by Eq. (18)

Update population

End while

Recall = best fitness value

weight = Solution corresponding to best fitness value

dimensions of shape features are 16, 6, and 2 extracted from the moment of invariants, reshape (Eccentricity, Solidity, Circularity), Zernike moment, respectively [18, 56]. Similarly, the first-order feature, GLCM, and DWT [18, 54] of texture features are extracted with dimensions of 8, 22, and 8.

Simulation and Result Analysis

Simulations and obtained results are arranged in three parts, which are discussed in the following way. In the first part, performance measures of database images (training images) are described. In the same way, performance measures have been calculated on non-database images (testing images) in the second part. Finally, a variability analysis of feature’s weight both for database and non-database images is performed. Standard performance metrics of CBIR system are precision and recall. The formula for calculating precision and recall values are described in the following Eqs. (19) and (20):

Optimization Parameter and Feature Extraction

In this study, the above-described objective function has been implemented to optimize weights through AHP for medical image features. Several pre-trials have been conducted to identify suitable parameters of the optimization algorithm. The parameters used in simulation work are listed in Table 3. For every specified optimization algorithm, the number of decision variables and the maximum number of iteration have been set as 03 and 50, respectively.

In the retrieval system, the individual features deal with their corresponding dimensions. The respective dimensions of the color feature are 9, 64, and 6 from the color histogram, color auto-correlogram, and color moments [18, 54, 55]. The

Table 3 Parameter considered during simulation

Methods	Parameters	Values considered
GA	Population size	5
	Mutation rate	0.3
	Swarm size	5
	Personal learning coefficient (C1)	1.5
PSO	Global learning coefficient (C1)	2.0
	Inertia weight (w)	1
	Inertia weight damping ratio	0.99
GWO	Search of agents	5
JAYA	Population size	5

$$\text{Precision} = \frac{\text{number of relevant images retrieved}}{\text{total number of retrieved images}} \quad (19)$$

$$\text{Recall} = \frac{\text{number of relevant images retrieved}}{\text{total number of relevant images in database}} \quad (20)$$

Performance Measure of Database Image (Training Images)

In Table 4, the average precision (AP) and average recall (AR) of OPWC (GA-AHP, PSO-AHP, GWO-AHP, and JAYA-AHP) have been calculated for 10 randomly selected images from each class of skin melanoma disease database (training images). The proposed method provides significant retrieval of similar images in the database. The mean of average precision and recall of all 23 different class categories belonging to the melanoma image database are calculated over window size 25. For GA-AHP 99.34% and 24.83%, precision and recall have been observed. Similarly, the precision of 99.77%, 99.74%, and 99.57% has been observed for PSO-AHP, GWO-AHP, and JAYA-AHP, respectively. Recall of 24.94%, 24.94%, and 24.89% has been observed for PSO-AHP, GWO-AHP, and JAYA-AHP, respectively.

Table 4 Average precision and recall of randomly chosen 10 images from each class of training database images using OPWC approaches

Class	GA-AHP		PSO-AHP		GWO-AHP		JAYA-AHP	
	AP	AR	AP	AR	AP	AR	AP	AR
1	95.2	23.8	95.6	23.9	97.6	24.5	99.6	24.9
2	98.8	24.7	100	25	100	25	100	25
3	100	25	100	25	100	25	100	25
4	99.2	24.8	100	25	100	25	100	25
5	98	24.5	99.2	24.8	99.2	24.8	99.2	24.8
6	99.2	24.8	100	25	100	25	100	25
7	100	25	100	25	100	25	100	25
8	100	25	100	25	100	25	100	25
9	100	25	100	25	100	25	98.6	24.6
10	99.2	24.8	100	25	99.2	24.8	98	24.5
11	98.4	24.6	100	25	98	24.5	100	25
12	98	24.5	100	25	100	25	98.8	24.7
13	100	25	100	25	100	25	100	25
14	100	25	100	25	100	25	100	25
15	100	25	100	25	100	25	100	25
16	100	25	100	25	100	25	100	25
17	100	25	100	25	100	25	100	25
18	100	25	100	25	100	25	100	25
19	100	25	100	25	100	25	100	25
20	100	25	100	25	100	25	100	25
21	98.8	24.7	100	25	100	25	96	24
22	100	25	100	25	100	25	100	25
23	100	25	100	25	100	25	100	25

Table 5 Average ranking of OPWC approaches based on precision and recall for training database images

Method	Rank based on precision and recall value	Rank
GA-AHP	2.913	IV
PSO-AHP	2.2174	I
GWO-AHP	2.3478	II
JAYA-AHP	2.5217	III

Table 5 concludes the statistical significance of obtained optimization results based on the Friedman average test. Here, the lower value indicates high rank. Friedman statistic assumes reduction performance of specified algorithms at a significance level, $\alpha = 0.05$. The ranking of optimized AHP algorithms is sorted in descending order as PSO-AHP, GWO-AHP, JAYA-AHP, and GA-AHP based on the precision and recall values.

Performance Measure of Non-Database Image (Testing Images)

The average precision (AP) and average recall (AR) of the OPWC approaches (GA-AHP, PSO-AHP, GWO-AHP, and

JAYA-AHP) have been calculated with randomly selected 10 images from each class of non-database from melanoma (testing images) shown in Table 6.

The proposed OPWC approach obtains better retrieval of similar images in non-database images. The mean of average precision and recall of all 23 different class categories belonging to non-database images are calculated over window size 25. For GA-AHP, 98.24% and 24.56% precision and recall have been observed. Similarly, the precisions of 99.15%, 98.77%, and 99.55% have been observed for PSO-AHP, GWO-AHP, and JAYA-AHP, respectively. Recall of 24.79%, 24.69%, and 24.88% has been observed for PSO-AHP, GWO-AHP, and JAYA-AHP respectively.

The statistical significance of achieved optimization results using the Friedman average ranking test is shown in Table 7. The ranking of OPWC algorithms is sorted in descending order as JAYA-AHP, PSO-AHP, GWO-AHP, and GA-AHP based on the precision and recall values.

From the result analysis, it is observed from Table 4 that the classes 1, 5, 10, 11, and 21 have images which are difficult to match with their similar images. These are the classes having images of acne and Rosacea, cellulitis impetigo, and other bacterial infections, light diseases, and disorders of pigmentation, lupus and other connective

Table 7 Average ranking of OPWC approaches based on precision and recall for testing (non-database) images

Method	Rank based on precision and recall value	Rank
GA-AHP	3.0217	IV
PSO-AHP	2.1957	II
GWO-AHP	2.7826	III
JAYA-AHP	2	I

tissue diseases, and vascular tumor types of skin melanoma. Furthermore, these classes may be targeted to increase the performance of overall system.

AHP-PSO approach performs better on training images, while from the results of testing images, it is observed that JAYA-AHP approach performs better. Here, it is concluded that JAYA optimization algorithm will be the better option in case of less number of images.

In Fig. 2, an illustration of the visual output for doctor’s assistance is shown as a CBMIR system. This fully automated assistance system helps the doctors and physicians to easily identify the type of disease and similar cases.

Table 6 Average precision and recall of randomly chosen 10 images from each class of testing database image (non-database) using OPWC approaches

Class	GA-AHP		PSO-AHP		GWO-AHP		JAYA-AHP	
	AP	AR	AP	AR	AP	AR	AP	AR
1	86.8	21.7	96.8	24.2	90.6	22.6	97.6	24.4
2	88.4	22.1	94	23.5	96	24	99.2	24.8
3	100	25	100	25	100	25	99.6	24.9
4	98.4	24.6	98.4	24.6	98	24.5	99.2	24.8
5	99.2	24.8	99.6	24.9	99.6	24.9	100	25
6	99.2	24.8	100	25	99.2	24.8	100	25
7	100	25	100	25	100	25	100	25
8	98.4	24.6	98.8	24.7	98.4	24.6	99.6	24.9
9	98	24.5	98.4	24.6	97.6	24.4	99.2	24.8
10	99.2	24.8	99.6	24.9	99.2	24.8	99.6	24.9
11	100	25	100	25	100	25	100	25
12	98.8	24.7	99.6	24.9	99.2	24.8	100	25
13	99.2	24.8	99.2	24.8	98.8	24.7	99.6	24.9
14	97.6	24.4	98	24.5	98.4	24.6	98.8	24.7
15	100	25	100	25	100	25	99.2	24.8
16	100	25	100	25	100	25	100	25
17	98.8	24.7	98.4	24.6	98.8	24.7	99.2	24.8
18	99.2	24.8	100	25	99.6	24.9	99.6	24.9
19	100	25	100	25	100	25	100	25
20	100	25	100	25	99.2	24.8	100	25
21	99.6	24.9	100	25	100	25	99.2	24.8
22	100	25	100	25	100	25	100	25
23	98.8	24.7	99.6	24.9	99.2	24.8	100	25



Fig. 2 Visual output of non-database image using optimized pair-wise approach JAYA-AHP

Analysis of Feature’s Weights

Automatic and dynamic weights of features for database image (training images) and non-database image (testing images) of proposed OPWC approaches (GA-AHP, PSO-AHP, GWO-AHP, and JAYA-AHP) are given in the supplementary file. The weights of color, shape, and texture features are represented as W_c , W_s , and W_t , respectively. The statistical measures like mean, variance, and standard deviation have been calculated and observed. For an easy observation, bar chart representations are shown in Figs. 3 and 4. In Figs. 3a and 4a, the corresponding mean

weight values in the database and non-database image, it is observed that the shape feature’s weight dominates other features based on the nature of the image. The shape feature specifies high weight importance through both the variance and standard deviation compared to others by applying three proposed OPWC approaches except JAYA-AHP for database images shown in Fig. 3b and c as well as non-database images shown in Fig. 4b and c, respectively. But, the color feature’s weight shows better for all types of images in variance and standard deviation with the implementation of JAYA-AHP approach found in Figs. 3b, c and 4b, c.

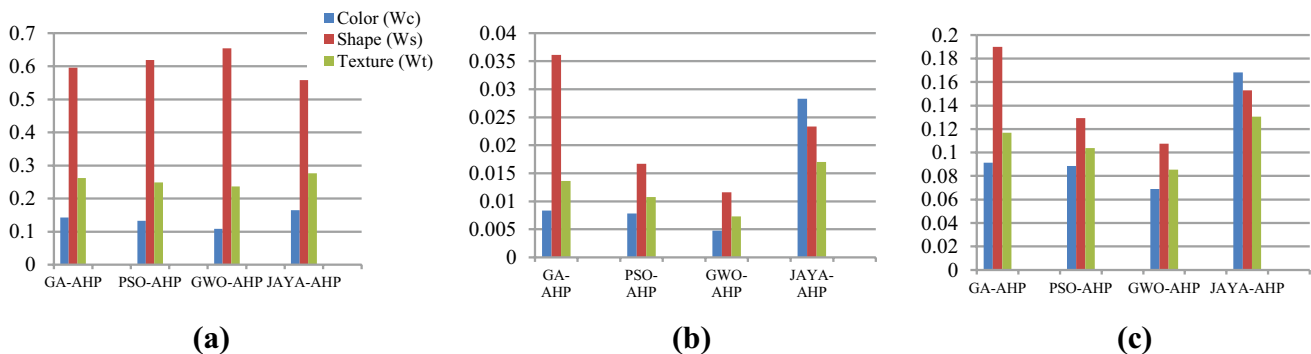


Fig. 3 Statistical analysis of feature weights for database image a Mean b Variance c Standard deviation

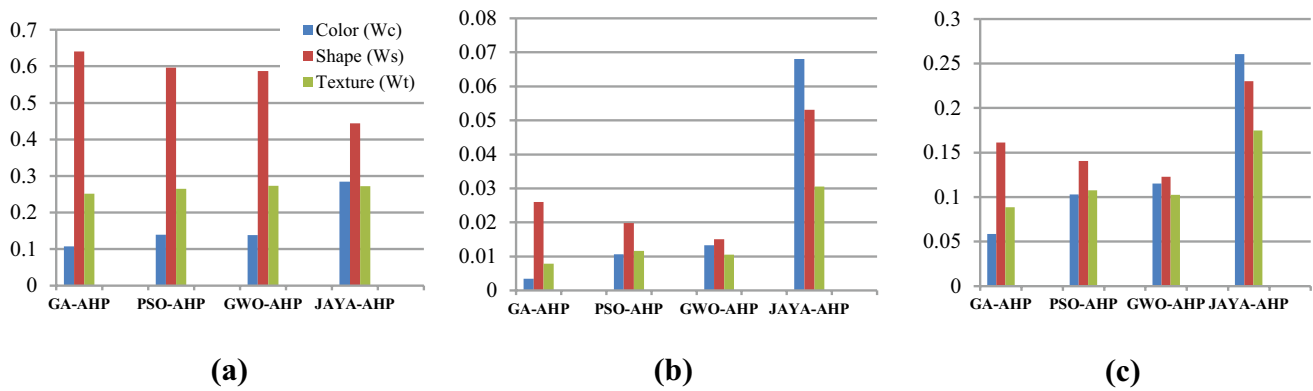


Fig. 4 Statistical analysis of feature weights for Non-database image a Mean b Variance c Standard deviation

Discussion

In general, the key concept of the CBMIR system is the classification of images based on feature extraction techniques. Mostly, the weight of the features of the image plays a vital role in classifying the images. If feature weights are not selected properly, then results may not be accurate. In this proposed CBMIR system for skin lesion melanoma database, training and testing images have been used for simulation of automatic and dynamic selection of feature weights. Here, medical image retrieval is performed with the help of dynamically determined optimal feature’s weight as per the nature of images. For an auto-determination of optimal feature weight, different OPWC approaches such as GA-AHP, PSO-AHP, GWO-AHP, and JAYA-AHP have been implemented. The proposed retrieval system is implemented over randomly selected training images and has been tested over randomly selected testing images of the database. Hence, the proposed system helps to assist doctors and physicians in identifying

the correct types of skin melanoma disease, and patients get proper treatment without error.

Table 8 is listed with the studies of similar kind with other state-of-the-art methods. Most of the studies use deep learning methods like CNN and concept of transfer learning for identification of different types of skin disease.

Limitations

Intensive computation that needs a bit longer time is limitation of the proposed approach. Online or real-time use of this approach may suffer from delay. Hence, it is required to explore other less computation-intensive optimization algorithm as alternative way.

Future Directions

Furthermore, the same proposed approach can also be applied to different areas such as hyper spectral and multi spectral image identification, military target detection,

Table 8 Comparative analysis of proposed OPWC with other similar studies

Reference	Method used	Dataset	Precision	Recall	Accuracy
Hossen et al. [31]	Convolution neural network (CNN) for classification	Skin disease custom image dataset for acne, eczema, and psoriasis	86%, 43%, and 60%	67%, 60%, and 60% (window size not mentioned)	–
Anand et al. [57]	Modified U-Net Architecture	PH2	–	–	97.6%
Anand et al. [58]	Transfer learning and pre-trained Xception model	HAM10000 (for Benign Keratosis)	99%	–	96.40%
Proposed approach	Optimal pair-wise comparison (OPWC) using JAYA-AHP	DermNet (Testing Images)	99.55%	24.88% (for window size 25)	–
Proposed approach	Optimal pair-wise comparison (OPWC) using PSO-AHP	DermNet (Testing Images)	99.15%	24.79% (for window size 25)	–

The bold entries only reflect "The proposed approach outperforms previous approaches"

missile launching and planning, and for other disease diagnosis. Optimization-based pair-wise comparison approach can also be applied on a different system known as Relevance Feedback-CBIR system. Different variants of AHP can also be used to make pair-wise comparison.

Conclusion

This paper presents an effective medical image retrieval system as an assistive tool for doctors. This may be very helpful to the healthcare industry. The unique quality of the proposed OPWC approach is that the weights assigned to the features of the searched image are automatic and dynamic. The proposed OPWC such as GA-AHP, PSO-AHP, GWO-AHP, and JAYA-AHP has been employed for automatic and dynamic determination of weights based on the contents of medical images. The developed model was tested with 23 categories of melanoma database and non-database images and delivering high retrieval accuracy. Among all OPWC approaches used, PSO and JAYA algorithm perform better compared to other listed algorithms for database images (Training images) and non-database images (Testing images), respectively. Hence, this image searching model can lead to the development of an expert system to help the physicians in identifying correct types of melanoma diagnosis and the patients in getting the right kind of treatment without any error.

Supplementary Information The online version contains supplementary material available at <https://doi.org/10.1007/s10278-022-00710-y>.

Acknowledgements The authors would like to thank the Department of Dermatology of the Hospital Clínic de Barcelona for the preparation of the ISIC Challenge 2018.

Author Contribution All the authors contributed to the study conception and design. We confirm that the manuscript has been read and approved by all the named authors and that there are no other persons who satisfied the criteria for authorship but are not listed. We further confirm that the order of authors listed in the manuscript has been approved by all of us.

Data Availability The datasets generated during and/or analyzed during the current study are available in the ISIC Challenge 2018 repository [Webpage: <http://www.dermnet.com/>, Direct link: <https://www.kaggle.com/shubhamgoel27/dermnet>].

Declarations

Ethics Approval Ethical approval not required for this study. Human or animal subjects' data is not used in this study.

Informed Consent Not applicable.

Conflict of Interest The authors declare no competing interests.

References

- Muller H, Michoux N, Bandon D, Geissbuhler A (2004) A review of content-based image retrieval systems in medical applications - Clinical benefits and future directions. *Int. J. Med. Inform.* 73(1): 1–23. <https://doi.org/10.1016/j.ijmedinf.2003.11.024>.
- Owais M, Arsalan M, Choi J, Park KR (2019) Effective Diagnosis and Treatment through Content-Based Medical Image Retrieval (CBMIR) by Using Artificial Intelligence. *Journal of clinical medicine* 8(4): 462. <https://doi.org/10.3390/jcm8040462>
- Miranda E, Aryuni M (2016) A Survey of Medical Image Classification Techniques. In 2016 International Conference on Information Management and Technology (ICIMTech). pp 56–61. <https://doi.org/10.1109/ICIMTech.2016.7930302>
- Ma L, Liu X, Gao Y, Zhao Y, Zhao X, Zhou C (2017) A new-method of content based medical image retrieval and its applications to CT imaging sign retrieval. *J. of Biomed. Inform.* 66: 148–158. <https://doi.org/10.1016/j.jbi.2017.01.002>
- Tang J, Aghaian S, Thompson I (2014) Guest editorial: computer-aided detection or diagnosis (CAD) systems. *IEEE Systems Journal* 8(3): 907–909. <https://doi.org/10.1109/JSYST.2014.2317378>.
- Lei Z, Fuzong L, Bo Z (1999) A CBIR method based on color-spatial feature, *IEEE Reg. 10 Annu. Int. Conf. Proceedings/TENCON 1*: 166–169. <https://doi.org/10.1109/TENCON.1999.818376>.
- Su Z, Zhang H, Li S, Ma S (2003) Relevance Feedback in Content-Based Image Retrieval: Bayesian Framework, Feature Subspaces, and Progressive Learning. *IEEE Trans. Image Process* 12(8): 924–937. <https://doi.org/10.1109/TIP.2003.815254>
- Swain MJ, Ballard DH (1991) Color Indexing. *International journal of computer vision* 32: 11–32. <https://doi.org/10.1007/BF00130487>.
- Huang J, Kumar SR, Mitra M, Zhu W-J, Zabih R (1997) Image indexing using color correlograms. *Proc. IEEE Comput. Soc. Conf. Comput. Vis. Pattern Recognit.* pp 762–768. <https://doi.org/10.1109/CVPR.1997.609412>
- Dudani SA, Breeding KJ, McGhee RB (1977) Aircraft Identification by Moment Invariants. *IEEE Trans. Comput.* 100(1): 39–46. <https://doi.org/10.1109/TC.1977.5009272>
- Mingqiang Y, Kidiyo K, Joseph R (2008) A survey of shape feature extraction techniques. *Pattern recognition* 15(7): 43–90. <https://hal.archives-ouvertes.fr/hal-00446037>
- Tsai HH, Chang B, Liou S (2014) Rotation-invariant texture image retrieval using particle swarm optimization and support vector regression. *Appl. Soft Comput.* 17: 127–139. <https://doi.org/10.1016/j.asoc.2013.12.003>.
- Haralick RM (1979) Statistical and structural approach to texture. *Proceeding IEEE* 67(5): 786–804. <https://doi.org/10.1109/PROC.1979.11328>
- Wang X-Y, Zhang B-B, Yang H-Y (2014) Content-based image retrieval by integrating color and texture features. *Multimed. Tools Appl.* 68(3): 545–569. <https://doi.org/10.1007/s11042-012-1055-7>
- Varish N, Pal AK (2018) A novel image retrieval scheme using gray level co-occurrence matrix descriptors of discrete cosine transform based residual image. *Appl. Intell.* 48(9) : 2930–2953. <https://doi.org/10.1007/s10489-017-1125-7>
- Ahirwal MK, Kumar A, Singh GK (2017) An Approach to Design Self Assisted CBIR System. *Proc. Int. Conf. Graph. Signal Process-ICGSP '17.* pp 21–25. <https://doi.org/10.1145/3121360.3121378>
- Rout NK, Ahirwal MK (2018) A Content Based Image Retrieval System: Analysis of Individual and Mixed Image Features, 2018 Inter. Conf. on Recent Innov. in Elec., Electronics & Comm. Engg. (ICRIEECE). pp 2561–2566. <https://doi.org/10.1109/ICRIEECE44171.2018.9009128>

18. Rout NK, Atulkar M, Ahirwal MK (2021) A Review on Content Based Image Retrieval System: Present Trends and Future Challenges. *International Journal of Computational Vision and Robotics* 11(5): 461–485. <https://doi.org/10.1504/IJCVR.2021.117578>
19. Cheng CH, Liu W-X (2018) Identifying Degenerative Brain Disease Using Rough Set Classifier Based on Wavelet Packet Method. *Journal of Clinical Medicine* 7(6): 124. <https://doi.org/10.3390/jcm7060124>
20. Murala S, Wu QMJ (2014) Local Mesh Patterns Versus Local Binary Patterns: Biomedical Image Indexing and Retrieval. *IEEE J. Biomed. Heal. Informatics* 18(3): 929–938. <https://doi.org/10.1109/JBHI.2013.2288522>
21. Zhang X, Liu W, Dundar M, Badve S, Zhang S (2014) Towards Large-Scale Histopathological Image Analysis : Hashing-Based Image Retrieval. *IEEE Transactions on Medical Imaging* 34(2): 496–506. <https://doi.org/10.1109/TMI.2014.2361481>
22. Liu X, Ma L, Song L, Zhao Y, Zhao X, Zhou C (2015) Recognizing Common CT Imaging Signs of Lung Diseases through a New Feature Selection Method based on Fisher Criterion and Genetic optimization. *IEEE J. Biomed. Health Informatics* 19(2): 635–647. <https://doi.org/10.1109/JBHI.2014.2327811>
23. Shinde A, Rahulkar A, Patil C (2019) Content based medical image retrieval based on new efficient local neighborhood wavelet feature descriptor. *Biomed. Eng. Lett.* 9(3): 387–394. <https://doi.org/10.1007/s13534-019-00112-0>
24. El-Naqa I, Yang Y, Galatsanos NP, Nishikawa RM, Wernick MN (2004) A Similarity Learning Approach to Content-Based Image Retrieval: Application to Digital Mammography. *IEEE Trans. Med. Imaging* 23(10): 1233–1244. <https://doi.org/10.1109/TMI.2004.834601>
25. Shyu C, Brodley CE, Kak AC, Kosaka A, Aisen AM, Broderick LS (1999) ASSERT : A Physician-in-the-Loop Content-Based Retrieval System for HRCT Image Databases. *Computer Vision and Image Understanding* 75(1-2): 111–132. <https://doi.org/10.1006/cviu.1999.0768>
26. Baldi A, Murace R, Dragonetti E, Manganaro M, Guerra O, Bizzi S, Galli L (2009) Definition of an automated Content-Based Image Retrieval (CBIR) skin lesions. *Biomedical engineering online* 10(1): 1–10. <https://doi.org/10.1186/1475-925X-8-18>
27. Renita DB, Christopher CS (2020) Novel real time content based medical image retrieval scheme with GWO-SVM, *Multimedia Tools and Applications* 1-17. <https://doi.org/10.1007/s11042-019-07777-w>
28. Shamna P, Govindan VK, Nazeer KAA (2019) Content based medical image retrieval using topic and location model. *J. Biomed. Inform.* 91: 103112. <https://doi.org/10.1016/j.jbi.2019.103112>
29. Anand V, Gupta S, Koundal D, Nayak SR, Nayak J, Vimal S (2022) Multi-class Skin Disease Classification Using Transfer Learning Model. *International Journal on Artificial Intelligence Tools* 31(02):2250029. <https://doi.org/10.1142/S0218213022500294>
30. Anand V, Gupta S, Koundal D, Nayak SR, Barsocchi P, Bhoi AK (2022) Modified U-NET Architecture for Segmentation of Skin Lesion. *Sensors* 22(3): 867. <https://doi.org/10.3390/s22030867>
31. Hossen MN, Panneerselvam V, Koundal D, Ahmed K, Bui FM, Ibrahim SM (2022) Federated machine learning for detection of skin diseases and enhancement of internet of medical things (IoMT) security. *IEEE journal of biomedical and health informatics.* <https://doi.org/10.1109/JBHI.2022.3149288>
32. Xiaoling W, Kanglin XIE (2011) Content-Based Image Retrieval Incorporating the AHP Method. *International Journal of Information Technology* 11(1) : 25–37. <http://citeseerx.ist.psu.edu/viewdoc/summary?doi=10.1.1.106.4726>.
33. Moussaoui F, Cherrared M, Akli M (2018) A genetic algorithm to optimize consistency ratio in AHP method for energy performance assessment of residential buildings-Application of top-down and bottom-up approaches in Algerian case study. *Sustainable Cities and Society* 42: 622–636. <https://doi.org/10.1016/j.scs.2017.08.008>
34. Awad GA, Sultan EI, Ahmad N, Ithnan N, Beg AH (2011) Multi-Objectives Model to Process Security Risk Assessment Based on AHP- Multi-Objectives Model to Process Security Risk Assessment Based on AHP-PSO. *Modern Applied Science* 5(3): 246. <https://doi.org/10.5539/mas.v5n3p246>
35. Nayak AK, Mishra BSP, Das H (2019) Computational intelligence in sensor networks, Edited by B. B. Mishra, Satchidanand Dehuri, and Bijaya Ketan Panigrahi. Springer, 2019
36. Younus ZS, Mohamad D, Saba T, Alkawaz MH, Rehman A, Al-Rodhaan M, Al-Dhelaan A (2015) Content-based image retrieval using PSO and k-means clustering algorithm. *Arab. J. Geosci.* 8(8) :6211–6224. <https://doi.org/10.1007/s12517-014-1584-7>
37. Jiji GW, Durairaj PJ (2015) Content-based image retrieval techniques for the analysis of dermatological lesions using particle swarm optimization technique. *Appl. Soft Comput. J.* 30: 650–662. <https://doi.org/10.1016/j.asoc.2015.01.058>
38. Huang PC, Tong LI, Chang WW, Yeh WC (2011) A two-phase algorithm for product part change utilizing AHP and PSO. *Expert Syst. Appl.* 38(7): 8458–8465. <https://doi.org/10.1016/j.eswa.2011.01.043>
39. Kumar A, Suwendu S (2019) Automated face retrieval using bag - of - features and sigmoidal grey wolf optimization. *Evol. Intell.* pp 1–12. <https://doi.org/10.1007/s12065-019-00213-w>
40. Wang S, Phillips P, Dong Z, Zhang Y (2018) Intelligent facial emotion recognition based on stationary wavelet entropy and Jaya algorithm. *Neurocomputing* 272: 668–676. <https://doi.org/10.1016/j.neucom.2017.08.015>
41. Satapathy SC, Rajinikanth V (2018) Jaya Algorithm Guided Procedure to Segment Tumor from brain MRI. *Journal of Optimization.* <https://doi.org/10.1155/2018/3738049>
42. Srikanth MV, Yadaiah N (2020) Optimal parameter tuning of Modified Active Disturbance Rejection Control for unstable time-delay systems using an AHP combined Multi-Objective Quasi-Oppositional Jaya Algorithm. *Applied Soft Computing* 86: 1058881. <https://doi.org/10.1016/j.asoc.2019.105881>
43. Codella NCF, Gutman D, Emre Celebi M, Helba B, Marchetti MA, Dusza SW, Kallou A, Liopyris K, Mishra N, Kittler H, Halpern A (2018) Skin Lesion Analysis Toward Melanoma Detection: A Challenge at the 2017 International Symposium on Biomedical Imaging (ISBI), Hosted by the International Skin Imaging Collaboration (ISIC), pp 168–172. <https://doi.org/10.1109/ISBI.2018.8363547>
44. Combalia M, Codella NCF, Rotemberg V, Helba B, Vilaplana V, Reiter O, Halpern AC, Puig S, Malvey J (2019) BCN20000: Dermoscopic Lesions in the Wild. [arXiv:1908.02288](https://arxiv.org/abs/1908.02288). <https://arxiv.org/abs/1908.02288>
45. Tschandl P, Rosendahl C, Kittler H (2018) The HAM10000 dataset, a large collection of multi-source dermatoscopic images of common pigmented skin lesions *Scientific Data*, 5(1): 1–9. <https://doi.org/10.1038/sdata.2018.161>
46. Cheng S, Chou T, Yang C, Chang H (2005) A semantic learning for content-based image retrieval using analytical hierarchy process. *Expert Systems with Applications* 28(3): 495–505. <https://doi.org/10.1016/j.eswa.2004.12.011>.
47. Saaty, Thomas L. "What is the analytic hierarchy process?." In *Mathematical models for decision support*, pp. 109–121. Springer, Berlin, Heidelberg, 1988.
48. Wang X, Nianzu L, Kanglin M (2008) A novel AHP-based image retrieval interface. *Chinese Control and Decision Conference*, pp 2334–2337. <https://doi.org/10.1109/CCDC.2008.4597741>
49. Yalcinoz T, Altun H, Uzam M (2001) Economic Dispatch Solution Using A Genetic Algorithm Based on Arithmetic Crossover. In *2001 IEEE Porto Power Tech Proceedings (Cat. No. 01EX502)*, 2:4. <https://doi.org/10.1109/PTC.2001.964734>

50. Mirjalili S, Mohammad S, Lewis A (2014) Advances in Engineering Software Grey Wolf Optimizer. *Adv. Eng. Software*, 69: 46–61. <https://doi.org/10.1016/j.advengsoft.2013.12.007>
51. Rao R (2016) Jaya: A simple and new optimization algorithm for solving constrained and unconstrained optimization problems. *International Journal of Industrial Engineering Computations* 7(1) : 19–34. <https://doi.org/10.5267/j.ijiec.2015.8.004>
52. Migallon H, Morenilla AJ, Sanchez-Romero JL (2018) Parallel improvements of the Jaya optimization algorithm. *Applied Sciences* 8(5) :819. <https://doi.org/10.3390/app8050819>
53. Mane SU, Narsingrao MR, Patil VC (2018) A many-objective Jaya algorithm for many-objective optimization problems. *Decision science letters* 7(4) : 567–582. <https://doi.org/10.5267/j.dsl.2017.11.001>
54. Rout NK, Atulkar M, Ahirwal MK (2021) Analytic hierarchy process-based automatic feature weight assignment method for content-based satellite image retrieval system. *Soft Computing*, 1–11.
55. Rout NK, Atulkar M, Ahirwal MK (2021) Identification of Similar Gastrointestinal Images through Content Based Image Retrieval System based on Analytical Hierarchical Process. In 2021 2nd International Conference on Range Technology (ICORT), pp. 1–6. IEEE, 2021.
56. Rout NK, Atulkar M, Ahirwal MK (2022) Assimilation of pairwise comparison method to decide weights of features based on the content of image. *International Journal of Information Technology and Decision Making* (1–26). <https://doi.org/10.1142/S0219622022500407>
57. Anand V, Gupta S, Koundal D (2022) Skin disease diagnosis: challenges and opportunities. In *Proceedings of Second Doctoral Symposium on Computational Intelligence* (pp. 449–459). Springer, Singapore. https://doi.org/10.1007/978-981-16-3346-1_63
58. Anand V, Gupta S, Koundal D (2022) Detection and Classification of Skin Disease Using Modified Mobilenet Architecture. *ECS Transactions* 107(1):5059. <https://doi.org/10.1149/10701.5059ecst>

Publisher's Note Springer Nature remains neutral with regard to jurisdictional claims in published maps and institutional affiliations.

Springer Nature or its licensor holds exclusive rights to this article under a publishing agreement with the author(s) or other rightsholder(s); author self-archiving of the accepted manuscript version of this article is solely governed by the terms of such publishing agreement and applicable law.